JMEPEG (2012) 21:202–207
DOI: 10.1007/s11665-011-9902-7

1059-9495/$19.00

Composition-Property Correlation in B_2O_3-SiO_2 Preform Rods Produced Using Modified Chemical Vapor Deposition Technique

Mohammad Islam and Muhammad Rizwan Saleem

(Submitted August 16, 2010; in revised form January 28, 2011)

Due to unique optical properties of high birefringent (Hi-Bi) fibers for sensing and coherent optical communications, there is a strong interest in process optimization at preform fabrication and fiber drawing stages. Boron-doped silica cladding acts as stress-applying part resulting in polarization properties of Hi-Bi fibers that are strongly dependent on chemical composition. Using modified chemical vapor deposition (MCVD) technique, B_2O_3-doped silica preform rods were synthesized under different precursor gas flow conditions. Qualitative information about B_2O_3-SiO_2 system composition was derived from etching behavior in nonbuffered HF solution and subsequent microstructural examination using scanning electron microscope. Significant degree of B_2O_3 incorporation was seen in case of high BCl_3:$SiCl_4$ ratio and mild oxygen-deficient processing conditions. Increasing the B_2O_3 content to ~26 mol% led to a corresponding increase in coefficient of thermal expansion (CTE) to a maximum value of 2.35 ppm/K. The value of refractive index (RI), on the other hand, was found to decrease with increased B_2O_3 incorporation. A qualitative correlation between B_2O_3 and SiO_2 system composition and physical properties such as CTE and RI was established.

Keywords advanced characterization, electron microscopy, electronic materials

1. Introduction

For sensor applications and coherent optical communications, optical fibers require different values of refractive index (RI) along two mutually orthogonal optical modes within the fiber core. This variation in RI values is referred to as birefringence and can be introduced through either tailored core/cladding geometry or presence of stress-applying parts (SAP) (Ref 1, 2). In the latter case, residual stresses arise from coefficient of thermal expansion (CTE) mismatch between different components of the cladding material (Ref 3). A large amount of birefringence makes the fiber insensitive to small birefringent fluctuations typically present in fibers due to inhomogeneities in geometry or mechanical perturbation.

The addition of B_2O_3 into the SiO_2 glass network not only lowers its RI value, but it also generates residual stresses due to B_2O_3/SiO_2 CTE mismatch during fiber drawing at high temperatures. Another important optical property is beat length which is the fiber length over which the phase difference between the fast and slow axes (due to changes in RI values) of transmitted light changes by 2π. At lower temperatures, CTE mismatch appears in a state of stress which corresponds to a reduction in beat length whereas, at high temperatures, the beat length increases with birefringence disappearing completely at about 600 °C (Ref 4). In silica-rich glass, the atomic effect (i.e., change in polarizability caused by distortion of electron shells of the atoms) is dominant over lattice effect arising from movement of atoms under tensile or compressive stresses. Dopants such as P_2O_5 reduce glass viscosity through significant changes in its RI value. The effect of adding P_2O_5 and GeO_2 on residual thermal stresses, RI profile, and in turn, optical anisotropy was investigated by Scherer (Ref 5).

Modified chemical vapor deposition (MCVD) technique is employed for separate synthesis of perform rods with germanium-doped core and boron-doped cladding. The latter acts as SAP, once these preform rods are drawn into optical fibers with certain geometries. It has been found that the chemical composition of SAP determines polarization properties of high birefringent (Hi-Bi) fibers at different wavelengths for sensing applications (Ref 6). The higher the B_2O_3 content, the larger will be the value of CTE, which implies that there is an upper limit for B_2O_3 content in the preform cladding rod. A study compared the field distributions for various SAP distances, dopant concentrations, and transmission loss characteristics as a function of distance between SAPs (Ref 7). Another study reported the stress difference distribution by optical retardation along two birefringent axes and compared it with data predicted using finite element method (Ref 8). Deposition rates as high as ~1.3 g/min were reported when changes in standard MCVD process parameters were made. These changes involved use of thin-walled glass tubes with high flow rates and a broad hot zone, coupling of the support

Mohammad Islam, School of Chemical & Materials Engineering (SCME), National University of Sciences & Technology (NUST), Sector H-12, Islamabad, Pakistan and Institut des Matériaux Jean Rouxel - IMN, Université de Nantes, CNRS, UMR 6230, 2 rue de la Houssinière, BP 32229, 44322 Nantes cedex 3, France; and **Muhammad Rizwan Saleem**, Department of Mathematics and Physics, University of Eastern Finland, Joensuu, Finland. Contact e-mails: mohammad.islam@gmail.com and mohammad.islam@scme.nust.edu.pk.

tube with cooling water downstream of the hot zone for increased deposition efficiencies, and water cooling for reduced equilibrium temperature and deposition length, use of helium gas to increase thermal diffusivity of gas stream (Ref 9, 10).

Through optimization of processing parameters such as power level, oxygen flow rate, or nitrogen uptake, the RI and CTE values of the resulting preform rod can be tailored (Ref 11). Careful control of dopant concentration inside the core has been reported to result in tailored RI values (Ref 12, 13). Additional benefits of doping are associated reduction in consolidation temperature during preform fabrication stage, viscosity, and glass transition temperature (Ref 14). Incorporation of fluorine and chlorine has also been found to cause variations in RI values due to the formation of Si-F and Si-Cl bonds (Ref 15). Similar to their bulk counterparts, silica thin films are amorphous, nonstoichiometric with a chemical formula SiO_x (where $0 < x < 2$), and have argon incorporation during deposition (Ref 16).

Owing to unique properties exhibited by Hi-Bi fibers, there is a large technological interest to optimize different steps of fiber manufacturing, i.e., preform fabrication and fiber drawing along with a proper material selection. No simple analytical method seems to exist to provide an insight into physical parameter changes for the study of such fibers. This article deals with optimization of composition property relationship for perform rods fabricated for Hi-Bi fiber applications. We present results from synthesis of B_2O_3-doped perform rods under different processing conditions. Qualitative information regarding chemical compositions of the samples was derived indirectly from etching behavior of surfaces with different B_2O_3 content. Physical properties such as CTE and RI values were determined experimentally and a correlation between B_2O_3 incorporation in silica matrix and the resulting physical properties was established.

2. Experiment

The chemical reagents $SiCl_4$ and BCl_3 (>99.99% purity, Sigma-Aldrich) were used as raw materials in liquid phase. These precursor species in vapor form were transported to the deposition chamber using oxygen as a carrier gas. The helium gas flow was maintained for efficient heat transfer and to facilitate densification, whereas Freon was used to remove few layers from inner substrate surface in order to avoid any impurities on the surface.

During MCVD process, the substrate glass tube (*F-300, Heraeus*, $2.5 \times 1.9 \times 100$ cm^3 in size) was clamped and rotated by means of a lathe machine (Nokia Preform Lathe), while heating of the tube to desirable reaction temperatures was carried out using a traversing flame. Initially, the silica substrate tube was heated under Cl_2 flow to ~1700-1800 °C, a step referred to as *fire polishing*. After that, the precursor species with specific flow rates and molar composition were introduced into the chamber, where reaction would occur resulting in the formation of SiO_2 and B_2O_3 particles that move downstream of the hot zone where wall temperature is less than the gas phase temperature. Thermophoretic deposition would occur on inside walls of the tube, whereas unreacted species and soot would be transported out of the chamber. During the process, the flow rates, reaction temperature, and pressure were monitored using mass flow controllers, pyrometer, and pressure gages. As the reaction and subsequent deposition continued, the inside diameter became smaller over time until it was completely filled. On heating at ~2200 °C, consolidation and collapse of the filled tube transformed the initially hollow substrate into a solid, transparent rod-like shape. The preform rods so obtained had diameter and length of the order of ~40 mm and 1.5-2.0 m, respectively.

Table 1 Precursor gas flow rates and molar ratios during preform rod synthesis via modified chemical vapor deposition process

ID	Precursor gas flow ratio $F_{BCl_3}:F_{SiCl_4}:F_{O_2}:F_{He}$, sccm	Molar composition $n_{BCl_3}:n_{SiCl_4}:n_{O_2}$	% O_2
R1	190:800:1500:1000	1:4.21:7.89:5.30	+59.1
R2	410:1500:1700:1520	1:3.63:4.12:3.70	−5.9
R3	230:1000:1870:1250	1:4.27:8.01:5.34	+59.6
R4	240:1050:1220:1020	1:4.34:5.04:4.20	−1.0
R5	390:1500:1700:1520	1:3.85:4.36:3.89	−4.2

The precursor gas flow composition and molar flow rates during synthesis are shown in Table 1. From the molar ratio and theoretical amount of O_2 needed for stoichiometric B_2O_3 and SiO_2 conversion, it was noticed that perform rod processing conditions were O_2 deficient (R2, R5), O_2 excess (R1, R3), or about the same as theoretically required (R4).

The surface topography of the polished and etched preform rod cross sections was carried out using scanning electron microscope (*JEOL JSM-6460*). After sectioning a disc-shaped piece using diamond saw cutter, the cross sections were prepared using successively fine grits up to 4000 mesh and polished with alumina slurry to a surface roughness of 1 μm or less. Some of the polished surfaces were etched in a nonbuffered 0.5 M HF solution for 10 min. Prior to SEM examination, a ~5-nm thick conductive layer of Au-Pd alloy was applied via sputtering.

The CTE values for preform rods were determined using push-rod dilatometer (Orton, 2010STD) setup that measured change in sample length as a function of temperature under controlled heating/cooling conditions. Prior to measurement, the dilatometer was calibrated using Al_2O_3 standard sample by heating at 3 °C/min to ~1000 °C. The RI profiles were generated and recorded using a narrow, circular polarized He-Ne laser beam of 30 μm diameter, 1.0 mW power, and 633 nm wavelength (*P104 Preform Analyzer*).

3. Results and Discussion

3.1 Compositional Analysis

Since energy dispersive x-ray analysis is sensitive to atomic number of the elements, reliable information about B_2O_3 content in silica cannot be obtained for data interpretation and investigation of any correlation with CTE and RI change as a function of specimen composition. Nevertheless, EDS analysis of sample R5 (not shown here) indicated elemental boron to be ~8.9 wt.% that corresponded to ~26 mol% B_2O_3. Thus, through a crude estimate, it can be concluded that maximum B_2O_3 incorporation was of the order of ~26 mol% for perform rod made under relatively high BCl_3:$SiCl_4$ flow ratio and oxygen-deficient processing conditions.

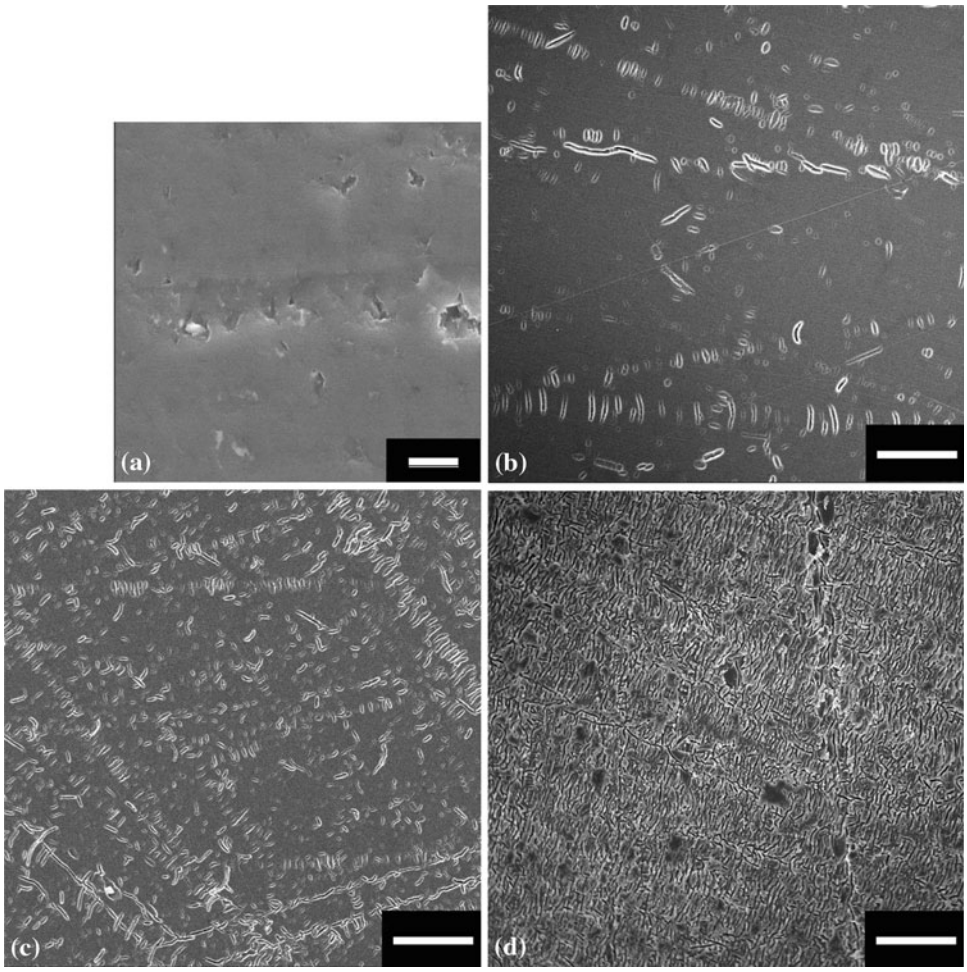

Fig. 1 SEM microstructures of the B_2O_3-SiO_2 preform rod cross sections: (a) polished surface (R2), (b) etched R4, (c) etched R1, and (d) etched R3. The scale bars in (a) and (b)-(d) represent lengths of 1 and 10 μm, respectively

To estimate the degree of B_2O_3 incorporation, an indirect approach was adopted involving etching behavior of B_2O_3-doped silica samples. The SEM images of the polished and etched surfaces are shown in Fig. 1. The polished surfaces appeared similar regardless of different incorporated B_2O_3 content, revealing an overall smooth surface with few scratches and surface pores formed during sample preparation step. The etched surfaces, however, appeared significantly different from each other due to different etching rates of SiO_2 and B_2O_3. Since the etching rate increases with an increase in B_2O_3 content when using nonbuffered HF solution (Ref 17), highly etched surfaces indicated greater extent of B_2O_3 incorporation in perform rods. For identical etching conditions, surfaces of samples R1, R3, and R4 revealed different topographies. On the etched R4 sample surface, finger-like pits of submicron width and lengths of the order of few microns were found to form as a result of etching. The area density of such etch features was relatively low, indicative of a low B_2O_3 content. Similar type of etch features, albeit with a higher number density, were observed in case of etched R1 sample.

From the size and distribution of etched features, qualitative information about homogeneity and extent of incorporated B_2O_3 can be inferred. Using nonbuffered HF solution was found to be very helpful in gaining insight into qualitative compositional analysis, since a direct correlation exists between B_2O_3 content and etch rate. On the other hand, etching with buffered HF solution shows opposite trends depending on the range of a B_2O_3 content in silica (Ref 18). SEM examination of the etched R3 sample surface indicated higher etch rate than both R1 and R4 implying greater B_2O_3 content than other samples. From etched surfaces, the sequence of samples with increasing B_2O_3 content was R4-R1-R3-R2-R5.

In the absence of any single technique that could yield reliable information regarding the composition of the perform rods, the combination of more than one ways to gain insight into the matter proved to be a very efficient method. This approach is unique in that it was not found to have been adopted before.

3.2 Coefficient of Thermal Expansion Data

During CTE tests, the change in perform rod length on heating was plotted as percent length change as a function of temperature. From graphical presentation of the data obtained for all samples, as shown in Fig. 2, a general trend toward change in CTE due to variation in perform rod composition could be inferred. The value of percent linear change (PLC) was observed to increase sharply on initial heating to ~350 K due to sudden change in glass temperature with a corresponding increase in kinetic energy of molecules. This rise in thermal

energy causes an increase in the vibrational amplitude of the molecules that form silica network, with consequent expansion. On further heating, all samples except R1 and R4 exhibited almost a linear behavior with a constant slope. The sample R1 was found to undergo an increase in slope resulting in a higher CTE value than sample R5. From the overall behavior of PLC versus *T*, it was deduced that sample R1 has a higher CTE value than that of R4. Such behavior maybe attributed to structural and/or phase transformation or separation in the silica glass network (Ref 19). From Fig. 2, it is evident that on increasing B_2O_3 content, the value of CTE increased to a maximum of 2.35 ppm/K. Since the CTE value for synthetic fused silica was determined to be ~0.13 ppm/K (not shown here), the findings suggest that even the sample with least B_2O_3 content had significant degree of B_2O_3 incorporation. Table 2 lists CTE values for all the preform rods with different B_2O_3-SiO_2 compositions.

3.3 Change in Refractive Index

Measurement of refractive indices at different translational locations provided information regarding homogeneity of incorporated B_2O_3 in the preform. In other words, the deposition characteristics of different regions inside the reaction zone were assessed in terms of change in RI. It also provided a sound basis for comparison of perform rods with different concentrations of B_2O_3 in silica. A typical profile of change in RI as a function of position along perform rod cross section is shown in Fig. 3. Depending on process conditions, either deficiency or excess of B_2O_3 content near the center of preform cross section was found to have occurred. A dip in RI profile at the center is caused by greater extent of B_2O_3 incorporation into silica network due to perfect sealing and complete blockage of evaporated B_2O_3 from the innermost layer during collapse step. On the other hand, B_2O_3 evaporation and its subsequent escape from reaction zone during final stages of deposition results in peak formation at the center of the RI profile. The magnitude of this central dip was reduced by using Freon gas at the initial collapse stage that has been reported to preferentially etch few microns of SiO_2 layer (Ref 20, 21).

Another prominent feature on the RI profile is the ripple-like behavior exhibited by the layers deposited near the center. This effect seemed to diminish in case of layers that had been deposited at the earlier stage of deposition. Since each layer has a finite thickness, each ripple represents one complete layer. The upper peak of any ripple indicates low B_2O_3 content at the outside perimeter of the layer and vice versa (Ref 13). For each preform, the RI value was measured from the RI profiler while ignoring the presence of any dip or peak near the center. Since $n_{B_2O_3} < n_{SiO_2}$, reduction in the RI value was observed as anticipated, due to B_2O_3 incorporation into the silica network. All samples indicated presence of a central dip characteristic of excess B_2O_3 content at the rod center. The order of increase in RI followed the same pattern as did the CTE values. The absolute values of RI change as well as RI values are listed in Table 2.

3.4 Correlation Between Composition and Physical Properties

By looking at the picture that emerged from the table of processing conditions, EDS data, and the etching behavior of the samples, it was noticed that increasing the BCl_3 flow rate even by small amounts while keeping the $SiCl_4$ and O_2 gas flow rates the same (as in case of samples R2 and R5), the competing reaction kinetics for B_2O_3 and SiO_2 formation changed significantly in favor of higher B_2O_3 incorporation into the perform rod. Similarly, comparison of samples R3 and R4, in terms of O_2 availability for B_2O_3 and SiO_2 formation, revealed that higher O_2 flow rate favors greater B_2O_3 content in the resulting perform.

Both CTE and RI change data pointed out to similar trends against different perform rod compositions. A direct correlation was found between B_2O_3 content in the perform rods and the

Table 2 Compositions of B_2O_3-doped preform rods against coefficient of thermal expansion (CTE) and refractive index (RI) data

ID	B_2O_3 content	CTE, 10^{-6}, K	RI change, 10^{-3}	Refractive index
R5	Maximum	2.35	7.9	1.4501
R2	Intermediate	1.91	7.1	1.4510
R3	Intermediate	1.48	7.0	1.4511
R1	Intermediate	1.40	6.8	1.4512
R4	Minimum	1.31	6.0	1.4520

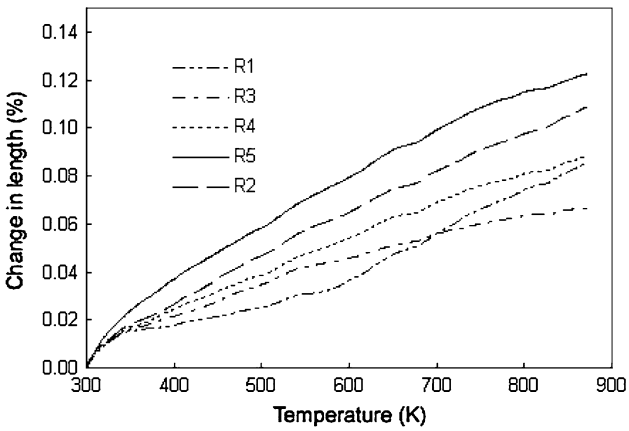

Fig. 2 Graphical representation of percent change in length as a function of temperature for different B_2O_3-SiO_2 preform rods

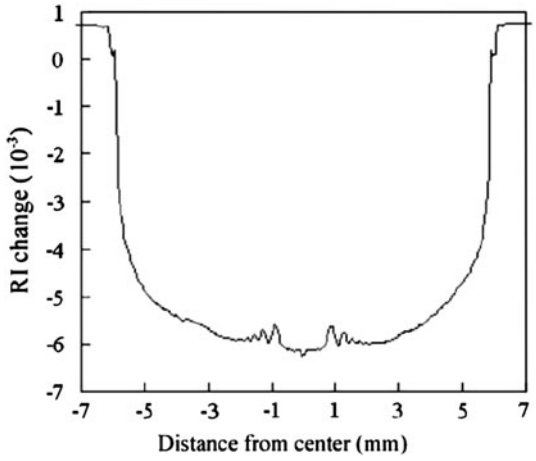

Fig. 3 Refractive index (RI) profile: change in RI value across the B_2O_3-SiO_2 preform rod cross section for sample R4

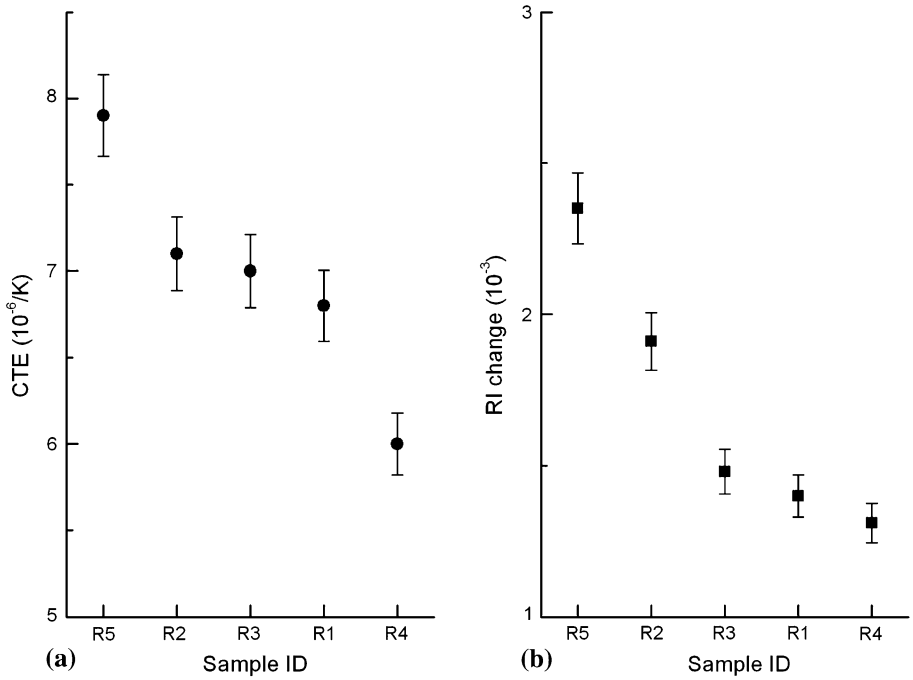

Fig. 4 Trends indicative of changes in (left) CTE and (right) RI values for different B_2O_3-SiO_2 preform rod compositions

resulting values of CTE and RI. It was noticed that increasing the B_2O_3 content in silica led to a corresponding increase in CTE value and a decrease in RI. The degree of B_2O_3 incorporation was estimated to be in the range of ~7-26% B_2O_3 by weight. Figure 4 shows an overall trend in change of these physical properties as a function of B_2O_3 content. A direct correlation between B_2O_3 content in perform rods and their respective CTE and RI values is clearly evident. A clear trend in change of values for these physical properties as a function of B_2O_3-SiO_2 composition, whether linear or exponential, cannot be discerned due to uncertainty in the exact composition of the perform rods.

From this study, few trends correlating processing conditions with the final composition and physical properties of the perform rods were found to have emerged: (a) An increase in total flow rate of the precursor gases, from ~2500 to 3600 sccm, led to an increase in B_2O_3 content. (b) For the same BCl_3:$SiCl_4$ flow ratio, increasing the O_2 flow rate, from 1220 to 1870 sccm, resulted in higher degree of B_2O_3 incorporation, and (c) helium flow rate had pronounced effect on the product characteristics as higher He flow rate of ~1500 sccm promoted greater B_2O_3 content due to more effective heating of the precursor gases. With the aid of more data obtained from diverse processing conditions and precise compositional analysis, an empirical relationship between precursor gas flow conditions and the resulting perform composition and physical properties can be developed.

4. Conclusions

The composition of B_2O_3-doped silica preform rods is very important since it dictates the values of important optical properties such as birefringence and beat length by acting as SAPs in a Hi-Bi fiber. In this study, the effect of processing parameters on composition and, in turn, the physical properties such as CTE and RI values was assessed. It was found that slightly oxygen-deficient conditions during MCVD process together with slightly higher BCl_3:$SiCl_4$ ratio lead to higher degree of B_2O_3 incorporation into silica matrix. Also, increasing the B_2O_3 content resulted in higher CTE value and reduction in RI to a greater extent. Such composition-property correlation can be exploited to tune processing conditions to obtain desirable materials compositions with appropriate physical properties for better performance in sensor and fiber optic applications.

References

1. O. Frazao, J.M. Baptista, and J.L. Santos, Recent Advances in High-Birefringence Fiber Loop Mirror Sensors, *Sensors*, 2007, **7**, p 2970–2983
2. X. Yu and P. Shum, Microstructured Fiber at 1550 nm with High-Birefringence Dispersion Compensation, *J. Optoelectron. Adv. Mater.*, 2005, **7**(6), p 3185–3190
3. F. Aranda, Asymmetry Maintains Polarization, *Laser Focus World*, 2002, **38**(5), p 187–190
4. A. Mendez and T. Morse, *Speciality Optical Fibers Handbook*, Academic Press, Boston, 2006
5. G.W. Scherer, Stress-Induced Index Profile Distortion in Optical Waveguides, *Appl. Opt.*, 1980, **19**(12), p 2000–2006
6. M. Alam, D. Guertin, J. Farroni, J. Abramczyk, N. Jacobson, and K. Tankala, Small Form-Factor PANDA type Hi-Bi Fiber for Sensing Applications, *Proc. SPIE 5272*, 2003
7. K. Tajima, M. Ohashi, and Y. Sasaki, A New Single-Polarization Optical Fiber, *J. Lightwave Technol.*, 1989, **7**, p 1499–1503
8. N. Shibata and M. Tokuda, Measurement of Stress Profiles in the Preform of a Polarization-Holding Fiber with Stress-Applying Parts, *J. Lightwave Technol.*, 1984, **2**(3), p 228–233
9. J.R. Simpson, J.B. MacChesney, K.L. Walker, and D.L. Wood, Physics of Fiber Optics, *Advances in Ceramics*, Vol II, B. Bendow and S.S. Mitra, Ed., 1981, p 8–13
10. M. Tsukamoto, K. Okamura, J. Goto, O. Nakamura, and T. Akamatsu, *Technical Digest IOOC*, San Francisco, CA, Paper WA2, 1981

11. R.H. Horng, F. Chen, D.S. Wuu, and T.Y. Lin, Refractive Index Behavior of Boron-Doped Silica Films by Plasma-Enhanced Chemical Vapor Deposition, *Appl. Surf. Sci.*, 1996, **92**, p 387–390
12. A.C. Ford, T. Tepper, and C.A. Ross, Reactive Pulsed Laser Deposition of Silica and Doped Silica Thin Films, *Thin Solid Films*, 2003, **437**, p 211–216
13. P. McNamara, K.J. Lyytikainen, T. Ryan, I.J. Kaplin, and S.P. Ringer, Germanium-Rich "Starburst" Cores in Silica-Based Optical Fibres Fabricated by Modified Chemical Vapour Deposition, *Opt. Commun.*, 2004, **230**, p 45–53
14. S.R. Negel, J.B. MacChesney, and K.L. Walker, An Overview of Modified Chemical Vapor Deposition Process and Performance, *IEEE Trans. Microw. Theory Tech.*, 1982, **30**(4), p 305–321
15. A. Chmel and V.N. Svetlov, Comparative Study of Incorporation of Cl and F into SiO_2 During the MCVD Process, *Opt. Mater.*, 1995, **4**, p 729–733
16. M. Islam and O.T. Inal, Synthesis and Characterization of Al_2O_3 and SiO_2 Films With Fluoropolymer Content using RF-Plasma Magnetron Sputtering Technique, *J. Vac. Sci. Technol. A*, 2008, **26**(5), p 198–204
17. S.J. Moss and A. Ledwith, *Chemistry of Semiconductor Industry*, Springer, New York, 1989, p 251
18. Y. Kunii, S. Nakayama, and M. Maeda, Wet Etching of Doped and Nondoped Silicon Oxide Films Using Buffered Hydrogen Fluoride Solution, *J. Electrochem. Soc.*, 1995, **142**(10), p 3510–3513
19. M.M. Lima and R. Monteiro, Characterisation and Thermal Behaviour of a Borosilicate Glass, *Thermochim. Acta*, 2001, **373**, p 69–74
20. S. Hopland, Removal of the Refractive Index Dip by an Etching Method, *Electron. Lett.*, 1978, **14**(24), p 757–759
21. M. Liegois, G. Lavanant, J.Y. Boniort, and C. Le Sergent, MCVD Preform Central Dip Reduction by Collapse Under Fluorinated Atmosphere, *J. Non-Cryst. Solids*, 1982, **47**(2), p 247–250